Peer-reviewed version available at *Remote Sens.* **2020**, *12*, 1748; doi:10.3390/rs12111748

Determining the Genetic Control of Common Bean Early-Growth Rate using Unmanned Aerial Vehicles

Travis A. Parker, Antonia Palkovic, and Paul Gepts*

Department of Plant Sciences / MS1, Section of Crop & Ecosystem Sciences, University of California, 1 Shields Avenue, Davis, CA 95616-8780, USA

* Correspondence: plgepts@ucdavis.edu; Tel.: +1-530-752-7743

ORCID

Paul Gepts https://orcid.org/0000-0002-1056-4665

Travis A. Parker https://orcid.org/0000-0002-1233-7829

Abstract

Vigorous early-season growth rate allows crops to compete more effectively against weeds and to conserve soil moisture in arid areas. Many crop species, including common bean, show genetic variation in growth rate between varieties. Despite this, the genetic basis of the early-season growth-related traits has not been well resolved in the species, in part due to historic phenotyping challenges. Using a range of UAV- and ground-based methods, we evaluated early-season growth vigor of two populations. These growth data were then used to find QTLs associated with several growth parameters. Our results suggest that early-season growth rate is the result of complex interactions between several genetic and environmental factors and highlight the need for the high-precision phenotyping provided by UAVs. The QTLs identified in this study are the first in common bean to be identified remotely using UAV technology and will be useful for developing crop varieties that compete with weeds more effectively. Ultimately, this will reduce crop losses and mitigate the need for herbicides and manual labor for weed control.

Keywords: Growth rate; vigor; UAV; sUAS; organic; weed competitiveness; *Phaseolus vulgaris*.

1. Introduction

Weeds are responsible for worldwide yield losses approximately equal to those incurred by all other pathogens and animal pests combined (Oerke 2005), and their control is a major economic and ecological burden. The competition between crops and weeds operates as a positive feedback loop, and advantages in resource capture early in the season allow one competitor to outcompete its neighbors for further resources. The strong positive effect of early-season growth rate on crop competitiveness against weeds has been studied in many major crops (van Bueren et al. 2011, Place et al. 2011, Manalil et al. 2017, Dass et al. 2017). These studies demonstrate that fast growth rate in both canopy area and canopy height are positively associated with weed competitiveness (Andrew et al. 2015).

In soybean, a grain legume grown globally for its oil- and protein-rich seeds, above-ground plant canopy area and canopy height are correlated with weed suppressive ability during the critical period for weed control (Place et al. 2011, Jannink et al. 2000, Bennett and Shaw 2000, Shilling et al. 1995, Jordan 1992). This vigorous early-season growth is critical for managing weeds while minimizing the use of herbicides and manual weeding. Average canopy coverage is also positively correlated with yield in soybean, therefore indicating that improving the trait may have a positive effect on final seed yield (Xavier et al. 2017). The effectiveness of improving yields through selection for the correlated trait of greater canopy coverage alone has recently been demonstrated (Moreira et al. 2019).

Despite the clear need for improved early-season growth rate across a range of crops, difficulties in evaluating the trait have been a major hindrance to its improvement. Traditionally, early-season growth vigor has been evaluated either visually using low-precision, high-throughput subjective methods (e.g., Sanchez-Valdez et al. 2004) or by a variety of high-precision, low-throughput methods (e.g., Sexton et al. 1997). These methods have been insufficient for determining precise values related to growth, while simultaneously being scalable to the level of large populations. Finally, environmental variables have a strong influence on early-season growth rate, so evaluations must be conducted over multiple years and field sites. This often translates into large costs associated with selecting for these traits and studying the genetic causes for their variation. Improved methods would be extremely useful for the evaluation of early-season growth rate.

The use of Unmanned Aerial Vehicles (UAVs, also known as sUAS or drones) has dramatically increased in recent years, due to improved technological and regulatory developments (Sankaran et al. 2015). These technological developments include improved mission planning software, superior aircraft performance, inexpensive high-precision sensors, and improved photogrammetry. Changes in UAV regulations, including part 107 remote pilot certification in the United States, has also made the use of UAVs more practical. Unlike traditional phenotyping approaches, the workload required for UAV-based phenotyping does not scale as a linear function of the number of plots in a trial. These methods are therefore well suited to large-scale evaluations targeting weakly heritable traits, such as growth rate. Previous UAV-based evaluations of soybean have successfully identified a major QTL for canopy cover on Gm19 (Xavier et al. 2017), which contains the *Dt1* allele for determinacy (Tian et al. 2010), although the two may not be precisely collocated. The use of UAV-based phenotyping methods will continue to grow as a major asset for plant genetics and breeding in the 21st century.

Common bean (*Phaseolus vulgaris* L.) is a nitrogen-fixing grain legume that has low fertilization requirements, breaks up pest and disease cycles for other crops, and improves soil structure. The species is the primary legume for direct human consumption and is a major source of nutrition for hundreds of millions of people globally (Gepts et al. 2008, Singh 1999). Consumption rates are highest in developing countries of the global south, where it serves as a major source of protein and micronutrition. In developed countries, there has been tremendous increases in dry bean production in the organic sector (USDA ERS, 2013), which is particularly limited in herbicide use. Organic growers often spend 2-5 times the amount on manual hand-weeding than their conventional counterparts (Klonsky 2011), and there is a strong demand for alternative means of control, such as through improved early-season vigor of the crop plant. Common bean varieties show variation in early-season growth rate. A more thorough understanding of this genetic diversity would be useful for improving weed competitiveness in the species.

2. Material and Methods

2.1. Plant Materials

The genetic basis of early-season growth rate was evaluated in two distinct populations. The first was the BeanCAP Middle American Diversity Panel (MDP, Moghaddam et al. 2016).

This population includes 280 varieties descended from the Middle American domestication event of *Phaseolus vulgaris* (Kwak et al. 2009). These varieties are indeterminate, with only 19 exceptions that have a determinate growth habit (7%; Singh 1982). This reduces any potential confounding effect of the large-impact but well-studied *PvTFL1y* and *PvTFL1z* mutations related to determinacy (Repinski et al. 2012; Kwak et al. 2012). In 2016, the population was grown in an unreplicated augmented design on transitional organic land in Sutter County, California (38.80° Lat., -121.64° Long.). In 2017 and 2018, two replicates of each variety in the population were grown on conventionally managed ground at the Plant Sciences Field Facility, UC Davis (38.53°, -121.78°). Seeds of all populations in all years were inoculated with Gard-N nitrogen fixing bacteria before planting.

A second population of 207 RILs was developed through reciprocal crosses between cultivar ‘Black Nightfall’ (W6 51267) and cultivar ‘Orca’ (PI 632344, Hang et al. 2003). Preliminary screenings of highly diverse heirloom and elite varieties in 2014 and 2015 had determined that Black Nightfall exhibited a more rapid growth rate than Orca. These varieties are both Middle American in ancestry and are indeterminate. Black Nightfall displays a type IIIb growth habit, with a large, viny, and somewhat prostrate canopy (Singh 1982). In contrast, Orca displays a small indeterminate type IIa growth habit (Singh 1982). This population (“BxO”) was grown in an augmented design each year for three years. Black Nightfall and Orca were among the controls for each block in the population. In 2017 and 2018, 30 seeds were planted in double-row 5ft x 5ft plots. In 2019, 120 seeds were planted in double-row 20ft x 5ft plots. All trials with this population were conducted on conventionally managed ground at the Plant Sciences Field Facility of UC Davis (38.53° Lat., -121.78° Long.).

2.2. Phenotyping

Both conventional and UAV-based methods (Fig. 1) were used to evaluate growth parameters. The number of plants emerging was hand-counted in each plot each year to correct for the effect of germination rate on plot growth rate metrics. UAV flights to evaluate growth rate were then conducted at 21, 28, 35, and 42 days after planting (DAP). This period represents a time of rapid canopy development in common bean. Starting around 42 days after planting, plants shifted resources into extensive reproductive development, such as flowers, fruits, and

seeds. Continued strong vegetative growth after this point may come at the cost of reproductive investment and is not clearly advantageous.

At each weekly evaluation, an UAV was flown over the field at an altitude of 17-20m. In 2016 and 2017, RGB imagery was captured using a DJI Phantom 3 12 MP stock camera with a Sony EXMOR 1/2.3 sensor. In 2017, multispectral imagery was collected using a Parrot Sequoia, and in 2018 and 2019 a Micasense RedEdge-M was used for multispectral imagery acquisition (Table 1). All images were captured automatically using Map Pilot (2016), Atlas Flight (2017), and DJI Ground Station Pro (2018, 2019) for mission planning, based on hardware compatibility (Table 1).

The ground sampling distance for all imagery was below 1.5cm/pixel (Table 1). Raw images from each flight were built into field-scale orthomosaics and digital surface models (DSMs) using Pix4Dmapper version 4.3.31. True-color orthomosaics were generated from RGB imagery and normalized difference vegetation index (NDVI, Rouse et al. 1974) orthomosaics were generated from multispectral imagery. Processed orthomosaics and DSMs were loaded into Quantum GIS ("QGIS") version 2.18 (QGIS Development Team 2018). The excess green (ExG, Woebbecke et al. 1995) vegetation index was calculated from true-color orthomosaics using the QGIS raster calculator function. ExG and NDVI rasters were then used for threshold-based image classification to distinguish canopy from soil. These classification layers were then used to make canopy-specific DSMs (cDSM, soil raster values filtered) and soil-specific DSMs (sDSM, canopy raster values filtered). The QGIS vector grid function was used as a high-throughput method to set up a grid of shapefiles over the field, with each shapefile covering the position of a single field plot. Percent canopy area, mean canopy elevation, maximum canopy elevation, and median soil elevation for each plot was then downloaded into the shapefiles' attribute tables using the zonal statistics plugin.

Attribute table data from the zonal statistics plugin were downloaded for final preparation. Mean and maximum canopy heights were generated by subtracting the median sDSM value for a plot (corresponding to the top of the soil bed) from the mean or maximum cDSM value of the same plot. QTL mapping and a genome-wide association study (GWAS) of canopy area-related traits were run with a correction for augmented design, although this correction was not used for height-related traits, where it typically reduced data quality and the significance of results. Emergence rate has a major effect on many growth rate metrics and was

variable among varieties and years. Variation in emergence was corrected in two ways. First, the number of hand-counted emerging plants was used to evaluate average growth on a per-plant basis. This correction is relatively conservative, as plots with low emergence rates face reduced competition from neighbors, and often display greater per-plant growth rates. The main emergence-correction method employed a locally weighted LOESS regression (Cleveland and Devlin 1988) between emergence and growth rate for the plots of each population and year. The residuals of each field plot from the Loess curve was used as an emergence-corrected phenotype for GWAS and QTL mapping.

UAV-based phenotyping was complemented by hand measurements and sampling. Canopy heights of plants at 42 days were taken for the MDP from 2016-2018, and canopy heights of the BxO population were taken at 42 and 63 days after planting in 2018 and 2019. Direct comparisons involving Black Nightfall and Orca were made by student's t-test with a significance threshold of 0.05.

2.3. Genotyping and genetic mapping

The MDP was genotyped using the Illumina BARCBean6K_3 BeadChip and Genotyping-by-Sequencing (GBS), as described previously (Moghaddam et al. 2016). The SNP data consisted of 211,763 markers. The data set was filtered to remove varieties not included in the original 280-member panel, and all SNPs with a minor allele frequency below 0.1 in this group were eliminated, leaving 81,337 final SNPs. Genotype data for the MDP can be found at: http://arsftfbean.uprm.edu/beancap/research/

GWAS of the MDP was conducted by generalized linear model in TASSEL (Bradbury et al. 2007) through the SNiPlay interface (Dereeper et al. 2011). A correction for population structure was performed using the first five principal components of the genetic data. Manhattan plots were visualized using the qqman R package (Turner 2018). A Bonferroni significance threshold was assigned based on a false-discovery rate of 0.05 (LOD=6.21) and included in all Manhattan plots.

In the BxO population, DNA was extracted from individual F8 seeds using a modified CTAB protocol. Quality was checked by gel and NanoDrop spectrophotometer, and the population was genotyped using the Illumina BARCBean6K_3 BeadChip (Song et al. 2015). A

total of 1,164 SNPs segregated between the parents and among the RILs. Linkage mapping was conducted in the ASMap R package (Taylor and Butler 2017), with a minimum linkage significance threshold between markers of 10-5. Composite interval mapping was performed using maximum likelihood through the EM algorithm in R/qtl (Lander and Botstein 1989, Broman et al. 2003). The 95th percentile of LOD scores of 1000 randomized permutations of the data (LOD=3.03) was used as a significance threshold.

3. Results

3.1. Growth measurements

Growth rate measurements between weeks were highly correlated, with correlation coefficients at times exceeding 0.9 (Fig. 2). Correlations were stronger between weekly data collection of canopy area (Fig. 2a-c) than those of canopy height (Fig. 2d-f). Canopy volume measurements were intermediate in correlation (Fig. 2g-i). Differences in these correlations also existed based on allele. Individuals with the lodging-associated allele S07_34512442_G (see Results section 3.2), for example, had relatively low correlations in height between 35 DAP and 42 DAP in the MDP in 2018 (R^2 = 0.33). In contrast, individuals with the alternate allele, associated with lodging resistance, had much higher predictability in height between in the same trial (R^2 = 0.73, Fig. 2f). Hand-measured and drone-measured canopy heights were also correlated (Fig. S1).

3.2. Genome-wide association studies

GWAS identified numerous loci associated with growth rate (Table S1), including at least two related to emergence-corrected canopy cover growth rate in the MDP (Fig. 3). One of these, on chromosome Pv01, was identified in 2016 when grown on organically managed land. A second locus, on Pv11 (LOD=6.19), approached the Bonferroni-corrected significance threshold (LOD=6.21). In 2018, a highly significant locus on Pv07 was identified when the population was grown in a conventional system. The most significant SNP from this GWAS was located at Pv07 position 34,512,442. GWAS of emergence rate failed to identify any significant SNPs in the MDP, although a locus on Pv06 was nearly significant (LOD=6.19) in 2018 (Fig. S2). GWAS of canopy height based on hand-measurements and drone-based methods each identified marker-

trait associations. In 2017, a peak on chromosome Pv01 in the vicinity of *PvTFL1y* was related to hand-measured height, while in 2018 loci on Pv07 and Pv08 played a significant role (Fig. S3). Drone-based height measurements identified a single SNP on Pv03 and a region of Pv05 that were related to the trait in 2017. In 2018, SNPs on Pv04 and Pv08 were related to canopy height (Fig. 4).

3.3.Biparental population phenotyping

Black Nightfall and Orca displayed statistically significant differences in several traits in the 2016-2019 trials (Table S2, Fig. S4). During the 21-42 DAP interval, Black Nightfall had a faster canopy coverage rate and simultaneously grew taller than Orca. The daily drone-measured increase in canopy area for plots of Black Nightfall surpassed those of Orca by 70% in 2016, 366% in 2017, 72% in 2018, and 247% in 2019. This difference was statistically significant in each year. During the same interval, Black Nightfall also grew taller in hand-measured canopy height, outcompeting Orca in each year from 2016-2019 by 36%, 26%, 18%, and 50% respectively. These differences were also statistically significant in each year. Drone-based height measurement also identified differences between Black Nightfall and Orca in 2017-2019, when multispectral imagery was used for DSM construction. Differences in the percentage of seeds that successfully germinated and emerged could have a strong influence on canopy-cover growth rate. In each year other than 2016, stand counts indicated that Black Nightfall had a significantly higher percentage of seedlings emerging than Orca. To correct for this, the average canopy cover growth rate per emerging plant was compared between varieties. In 2016, 2017, and 2019, Black Nightfall had a statistically significantly faster growth rate per plant than Orca, despite having greater between-plant competition because of its higher emergence rate. In 2018, Black Nightfall again had greater average per-plant canopy cover growth than Orca, although the difference was not significant (p=0.06).

3.4.Linkage map development and QTL analysis

A linkage map consisting of 730 SNPs was used to identify marker-trait associations in the BxO population (Fig. S5). This map consisted of 11 linkage groups that were arranged to match the numbers and direction of the chromosomes agreed upon by the *Phaseolus* community (Pedrosa-Harand et al. 2008). The linkage map was comparable in size to others in the species at

1138 cM. Individual chromosomes ranged from 64 cM to 132 cM, with between 41 and 109 markers. Average space between markers was 1.6 cM, with a maximum distance of 26 cM.

QTL mapping in the population identified regions associated with drone-measured canopy height, hand-measured canopy height, and canopy cover growth rate, using a residual from a LOESS model as an emergence correction (Table S3). QTL mapping identified three loci associated with canopy cover growth rate. The most significant of these was found on chromosome Pv07 in 2019 (Fig. 5). A locus on Pv06 was related to the trait in 2017 and 2018. Average seedling emergence was low in 2017 (32%) and 2019 (61%), but relatively high in 2018 (85%). QTL mapping for emergence rate showed that a major locus on Pv10 was the primary regulator of growth rate in 2017 and 2019, when emergence was low. In contrast, in the more favorable conditions of 2018, variation in emergence was related to a locus on chromosome Pv07 (Fig. S6).

Several QTLs were related to plant height in the BxO population. In all three years, chromosome Pv09 was significantly related to drone-measured maximum canopy height at 42 DAP (Fig. 6). In 2017 and 2019, another QTL was identified with a significant role on Pv10. A major QTL for hand-measured height 42 DAP was identified on Pv07 in 2018, while a secondary locus on Pv01 was also weakly significant (Fig. S7). Lodging scores taken simultaneously identified the same QTL, indicating that the variation in canopy height was likely the result of changes in canopy architecture. Hand-measurements of canopy height did not find a significant QTL on Pv07 at 42 DAP in 2019, while QTLs on Pv09 and Pv10 contained significant QTLs (Fig. S7). By 63 DAP in 2019, hand-measured canopy height measurements indicated that Pv07 was significantly associated with height in the population, while the role of the other chromosomes was reduced (Fig. S7).

4. Discussion

The QTLs identified in this work will be useful for improving the weed competitiveness of common bean. The most significant SNP from GWAS of the MDP was associated with canopy growth rate and was located at position 34,512,442 on Pv07, approximately 3kb from a SNP identified by Moghaddam et al. (2016) at position 34,509,509 in their evaluation of canopy

architecture. The SNP identified by Moghaddam et al. is predicted to cause a non-synonymous S740T mutation in the CDS of Phvul.007G221800. The SNP most strongly related to MDP canopy growth rate in this study was in the 5' UTR of the same gene model. Phvul.007G221800 is predicted to encode a leucine-rich repeat receptor-like protein kinase. Closely related members of this gene family include a BRASSINOSTEROID INSENSITIVE 1 precursor (transcript 29904.m003011) in *Ricinus communis* L. (Moghaddam et al. 2016). BRASSINOSTEROID INSENSITIVE 1 proteins are membrane-bound receptors of brassinolides, which regulate plant growth. Mutations in these genes cause severe growth stunting when mutated in *Arabidopsis thaliana* (L.) Heynh. (Clouse, 2002). In common bean, this locus pleiotropically regulates several characteristics, possibly by controlling plant stem length and flexuosity, which contribute to lodging. The most significant Pv07 growth rate SNP from the MDP is also within 800kb of *PvTFL1z*, a locus believed to control determinacy in Michigan-type small, white-seeded beans (Phvul.007G229300, Kwak et al. 2008, 2012, Nascimento et al. 2018). Identifying the polymorphisms responsible for this variation could be useful for improving canopy characteristics of common bean. Loci controlling seedling emergence, growth rate, and height on other chromosomes will also be strong candidates for continued genetic evaluation. These detailed molecular characterizations will parallel recent studies on other traits in the species, such as determinacy (Repinski et al. 2012), seed pigmentation (McClean et al. 2018), photoperiod sensitivity (Weller et al. 2019), and pod shattering (Parker et al. 2020).

Drone- and hand-measurement of plant height each yielded significant QTLs in the BxO population, but the loci and significance of these differed (Fig. 6, Fig S7). Drone-based methods identified highly significant QTLs for maximum canopy height on Pv09 in all three years, providing strong evidence that this chromosome is involved in the variation in plant height between Orca and Black Nightfall. Similarly, Pv10 included maximum height QTLs in two of three years. These chromosomes did not have significant QTLs when the same techniques were applied in the MDP, indicating that some of the responsible alleles may be at low frequency among Middle American beans, or may have complex interactions with other loci. In agreement with the drone-measured results, manual height measurements identified loci on Pv09 and Pv10 in 2019. In 2018, the major locus controlling hand-measured height was on Pv07, the chromosome associated with lodging and canopy area growth rate. The differences between drone- and hand-height measurement may be due partially to subtle differences in the precise

trait being measured. Hand-based height measurements took the height from the soil to the typical canopy level of a plot, whereas drone-based canopy heights measured the distance from the soil to the highest position of the digital surface model in the plot. While these models typically did not have sufficient resolution to capture individual guides (runners), they are much more sensitive to individual tall plants. If most but not all plants in a plot had lodged, the hand-measured height would be reduced, while the drone-based height measurement would continue to measure the height of the tallest plants. This could explain why the drone-based maximum height measurement methods did not identify the lodging locus on Pv07, but more consistently identified the loci on Pv09 and Pv10.

Plant growth is a complex phenomenon, influenced by interactions between numerous genetic and environmental factors. This phenotypic complexity requires multiple years of field evaluations to effectively identify loci that regulate traits of interest. Our results indicate that many factors, including emergence rate, genotype, and environmental differences interact to produce a range of growth-related traits. The role of some chromosomes and QTLs are fairly robust and can be identified in multiple populations and years. The role of other QTLs may only be of major importance in a narrower combination of environmental conditions and genetic backgrounds. In contrast to the relatively stable effects of the Pv07 locus found by Moghaddam et al. (2016) and in this study, Resende et al. (2018) did not identify any loci on Pv07 associated with canopy architecture. In their population, which consisted of 115 Middle American, 66 Andean, and seven admixed types, major lodging and architecture QTLs on Pv01 (possibly related to *PvTFL1y*, Repinski et al. 2012; Kwak et al. 2008) and Pv08 controlled trait variation. This highlights the importance of evaluating germplasm across a broad array of locations and environments.

Our results validate the utility of UAV in identifying QTLs in common bean. These are the first QTLs identified in this species using UAV-based imagery, although UAVs have been used for other purposes in the species (Trapp et al. 2016, Sankaran et al. 2018, Zhou et al. 2018, Sankaran et al. 2019). Use of UAVs to identify genetic variation will likely grow in the future as a complement to existing phenotyping methods. Further advances in UAV-related hardware and software will be of central importance for attaining these results. Improved sensor spectral resolution, photogrammetric algorithms, and data extraction tools will be of central importance

for improving UAV-based phenotyping. The remotely identified QTLs described here are likely to be the first of many found in common bean.

Characterizing the loci responsible for vigorous early-season growth is an important task. The identification of genetic regions controlling this trait will allow for the development of cultivars that compete with weeds more efficiently. In turn, this will help reduce the amount of manual and chemical weed control required for production of this major crop species. Ultimately, an improved understanding of this trait will have repercussions for farm profitability, labor availability, pesticide use, and ecological health for communities around the globe.

Author contributions: T.A.P. prepared the manuscript and conducted field trials, drone flights, photogrammetry, geospatial data extraction, GWAS, linkage mapping, and QTL mapping. A.P. assisted with field trials. P.G. conceived the initial project, assisted with manuscript preparation, and provided overall guidance.

Funding: Funding for TAP was provided through a Clif Bar Family Foundation Seed Matters fellowship and Lundberg Family Farm research support, with additional research funding from Western SARE and the UC Davis Plant Sciences Department.

Acknowledgements: Seeds of the ADP and MDP were provided by R. Lee and P. McClean (North Dakota State University). Undergraduates Natalie Hamada, Emily Yang, Ariel Herrera, Jose Pimentel, Matthew Bustamante, Emily White, Julia Gonzales, Paige Augello, Vivian Wu, Nathalie Gonzalez, and Aung Nyein contributed to field management and phenotyping. Jorge C. Berny Mier y Teran offered suggestions related to GWAS, linkage mapping, and QTL mapping. Taylor Nelson and Alex Mandel provided suggestions for geospatial methods; Umair Gull collaborated on developing UAV techniques.

Conflicts of Interest: The authors declare no competing interests. The funding sponsors had no role in the design of the study; in the collection, analyses, or interpretation of data; in the writing of the manuscript; or in the decision to publish the results.

References

Andrew IKS, Storkey J, Sparkes DL (2015) A review of the potential for competitive cereal cultivars as a tool in integrated weed management. Weed Research 55:239-248. https://doi.org/10.1111/wre.12137

Bennett AC, Shaw DR (2017) Effect of *Glycine max* cultivar and weed control on weed seed characteristics. Weed Science 48:431-435. https://doi.org/10.1614/0043-1745(2000)048[0431:EOGMCA]2.0.CO;2

Bradbury PJ, Zhang Z, Kroon DE, Casstevens TM, Ramdoss Y, Buckler ES (2007) TASSEL: software for association mapping of complex traits in diverse samples. Bioinformatics 23:2633-2635. https://doi.org/10.1093/bioinformatics/btm308

Broman KW, Wu H, Sen Ś, Churchill GA (2003) R/qtl: QTL mapping in experimental crosses. Bioinformatics 19:889-890. https://doi.org/10.1093/bioinformatics/btg112

Cleveland WS, Devlin SJ (1988) Locally weighted regression: An approach to regression analysis by local fitting. Journal of the American Statistical Association 83:596-610. https://doi.org/10.1080/01621459.1988.10478639

Clouse SD (2002) Brassinosteroid signal transduction: Clarifying the pathway from ligand perception to gene expression. Molecular Cell 10:973-982. https://doi.org/https://doi.org/10.1016/S1097-2765(02)00744-X

Dass A, Shekhawat K, Choudhary AK, Sepat S, Rathore SS, Mahajan G, Chauhan BS (2017) Weed management in rice using crop competition-a review. Crop Protection 95:45-52. https://doi.org/https://doi.org/10.1016/j.cropro.2016.08.005

Dereeper A, Nicolas S, Le Cunff L, Bacilieri R, Doligez A, Peros J-P, Ruiz M, This P (2011) SNiPlay: a web-based tool for detection, management and analysis of SNPs. Application to grapevine diversity projects. BMC Bioinformatics 12:134. https://doi.org/10.1186/1471-2105-12-134

Gepts P, Aragão FJL, Barros Ed, Blair MW, Brondani R, Broughton W, Galasso I, Hernández G, Kami J, Lariguet P, McClean P, Melotto M, Miklas P, Pauls P, Pedrosa-Harand A, Porch T, Sánchez F, Sparvoli F, Yu K (2008) Genomics of *Phaseolus* beans, a major source of dietary protein and micronutrients in the Tropics. In: Moore PH, Ming R (eds) Genomics of Tropical Crop Plants. Springer, Berlin, pp 113-143

Hang AN, Silbernagel MJ, Miklas PN (2003) Registration of 'Orca' black-and-white mottled Anasazi-type dry bean. Crop Science 43:1882-1882. https://doi.org/10.2135/cropsci2003.1882

Jannink JL, Orf JH, Jordan NR, Shaw RG (2000) Index selection for weed suppressive ability in soybean Crop Science 40:1087-1094. https://doi.org/10.2135/cropsci2000.4041087x

Jordan N (1992). Differential interference between soybean (*Glycine max*) varieties and common cocklebur (*Xanthium strumarium*): a path analysis. *Weed science*, *40*(4), 614-620.

Klonsky K (2011) Comparison of production costs and resource use for organic and conventional production systems. American Journal of Agricultural Economics 94:314-321. https://doi.org/10.1093/ajae/aar102

Kwak M, Kami JA, Gepts P (2009) The putative Mesoamerican domestication center of *Phaseolus vulgaris* is located in the Lerma-Santiago basin of Mexico. Crop Science 49:554-563. https://doi.org/10.2135/cropsci2008.07.0421

Kwak M, Toro O, Debouck D, Gepts P (2012) Multiple origins of the determinate growth habit in domesticated common bean (*Phaseolus vulgaris* L.). Annals of Botany 110:1573-1580. https://doi.org/10.1093/aob/mcs207

Kwak M, Velasco DM, Gepts P (2008) Mapping homologous sequences for determinacy and photoperiod sensitivity in common bean (*Phaseolus vulgaris*). J Hered 99:283-291. https://doi.org/doi:10.1093/jhered/esn005

Lammerts van Bueren ET, Jones SS, Tamm L, Murphy KM, Myers JR, Leifert C, Messmer MM (2011) The need to breed crop varieties suitable for organic farming, using wheat, tomato and broccoli as examples: A review. NJAS - Wageningen Journal of Life Sciences 58:193-205. https://doi.org/https://doi.org/10.1016/j.njas.2010.04.001

Lander ES, Botstein D (1989) Mapping Mendelian factors underlying quantitative traits using RFLP linkage maps. Genetics 121:185-199. https

Manalil S, Coast O, Werth J, Chauhan BS (2017) Weed management in cotton (*Gossypium hirsutum* L.) through weed-crop competition: A review. Crop Protection 95:53-59. https://doi.org/https://doi.org/10.1016/j.cropro.2016.08.008

McClean PE, Bett KE, Stonehouse R, Lee R, Pflieger S, Moghaddam SM, Geffroy V, Miklas P, Mamidi S (2018) White seed color in common bean (*Phaseolus vulgaris*) results from

convergent evolution in the *P* (pigment) gene. New Phytologist 219:1112-1123. https://doi.org/doi:10.1111/nph.15259

Moghaddam SM, Mamidi S, Osorno JM, Lee R, Brick M, Kelly J, Miklas P, Urrea C, Song Q, Cregan P, Grimwood J, Schmutz J, McClean PE (2016) Genome-wide association study identifies candidate loci underlying agronomic traits in a Middle American diversity panel of common bean. The Plant Genome 9:3. https://doi.org/10.3835/plantgenome2016.02.0012

Moreira FF, Hearst AA, Cherkauer KA, Rainey KM (2019) Improving the efficiency of soybean breeding with high-throughput canopy phenotyping. Plant Methods 15:139. https://doi.org/10.1186/s13007-019-0519-4

Nascimento M, Nascimento ACC, Silva FFe, Barili LD, Vale NMd, Carneiro JE, Cruz CD, Carneiro PCS, Serão NVL (2018) Quantile regression for genome-wide association study of flowering time-related traits in common bean. PLOS ONE 13:e0190303. https://doi.org/10.1371/journal.pone.0190303

Oerke EC (2005) Crop losses to pests. The Journal of Agricultural Science 144:31-43. https://doi.org/10.1017/S0021859605005708

Parker TA, Berny Mier y Teran JC, Palkovic A, Jernstedt J, Gepts P (2020) Pod indehiscence is a domestication and aridity resilience trait in common bean. New Phytologist 225:558-570. https://doi.org/10.1111/nph.16164

Pedrosa-Harand A, Porch T, Gepts P (2008) Standard nomenclature for common bean chromosomes and linkage groups. Annual Report of the Bean Improvement Cooperative 51: 106-107.

Place GT, Reberg-Horton SC, Carter TE, Brinton SR, Smith AN (2011) Screening tactics for identifying competitive soybean genotypes. Communications in Soil Science and Plant Analysis 42:2654-2665. https://doi.org/10.1080/00103624.2011.614040

QGIS Development Team (2018) QGIS Geographic Information System, http://qgis.osgeo.org. Open Source Geospatial Foundation Project

Repinski SL, Kwak M, Gepts P (2012) The common bean growth habit gene *PvTFL1y* is a functional homolog of *Arabidopsis TFL1*. Theoretical and Applied Genetics 124:1539-1547. https://doi.org/10.1007/s00122-012-1808-8

Resende RT, de Resende MDV, Azevedo CF, Fonseca e Silva F, Melo LC, Pereira HS, Souza TLPO, Valdisser PAMR, Brondani C, Vianello RP (2018) Genome-wide association and regional heritability mapping of plant architecture, lodging and productivity in *Phaseolus vulgaris*. G3: Genes|Genomes|Genetics 8:2841-2854. https://doi.org/10.1534/g3.118.200493

Rouse JW, Haas RH, Schell JA, Deering DW (1974) Monitoring vegetation systems in the Great Plains with ERTS. Third Earth Resources Technology Satellite-1 Symposium. Volume I: Technical Presentations, Section A, pp. 309-318. NASA special publication, Goddard Space Flight Center, Washington, D.C.

Sanchez-Valdez I, Acosta-Gallegos JA, Ibarra-Perez FJ, Rosales-Serna R, Singh SP (2004) Registration of 'Pinto Saltillo' common bean. Crop Science 44:1865-a-1866. https://doi.org/10.2135/cropsci2004.1865a

Sankaran S, Khot LR, Espinoza CZ, Jarolmasjed S, Sathuvalli VR, Vandemark GJ, Miklas PN, Carter AH, Pumphrey MO, Knowles NR, Pavek MJ (2015) Low-altitude, high-resolution aerial imaging systems for row and field crop phenotyping: A review. European Journal of Agronomy 70:112-123. https://doi.org/https://doi.org/10.1016/j.eja.2015.07.004

Sankaran S, Quirós JJ, Miklas PN (2019) Unmanned aerial system and satellite-based high resolution imagery for high-throughput phenotyping in dry bean. Computers and Electronics in Agriculture 165:104965. https://doi.org/https://doi.org/10.1016/j.compag.2019.104965

Sankaran S, Zhou J, Khot LR, Trapp JJ, Mndolwa E, Miklas PN (2018) High-throughput field phenotyping in dry bean using small unmanned aerial vehicle based multispectral imagery. Computers and Electronics in Agriculture 151:84-92. https://doi.org/https://doi.org/10.1016/j.compag.2018.05.034

Sexton PJ, Peterson CM, Boote KJ, White JW (1997) Early-season growth in relation to region of domestication, seed size, and leaf traits in common bean. Field Crops Research 52:69-78. https://doi.org/https://doi.org/10.1016/S0378-4290(96)03452-1

Shilling DG, Brecke BJ, Hiebsch C, MacDonald G (1995) Effect of soybean (*Glycine max*) cultivar, tillage, and rye (*Secale cereale*) mulch on sicklepod (*Senna obtusifolia*). Weed Technology 9:339-342. https://doi.org/10.1017/S0890037X00023447

Singh SP (1982). A key for identification of different growth habits of *Phaseolus vulgaris* L. Annual Report of the Bean Improvement Cooperative 25: 92-95

Singh SP, (ed.) (1999) Common bean improvement in the twenty-first century. Springer-Science+Business Media

Song Q, Jia G, Hyten DL, Jenkins J, Hwang E-Y, Schroeder SG, Osorno JM, Schmutz J, Jackson SA, McClean PE, Cregan PB (2015) SNP assay development for linkage map construction, anchoring whole-genome sequence, and other genetic and genomic applications in common bean. G3: Genes|Genomes|Genetics 5:2285-2290. https://doi.org/10.1534/g3.115.020594

Taylor J, Butler D (2017) R Package ASMap: efficient genetic linkage map construction and diagnosis. Journal of Statistical Software 79:1-29. https://doi.org/10.18637/jss.v079.i06

Tian Z, Wang X, Lee R, Li Y, Specht JE, Nelson RL, McClean PE, Qiu L, Ma J (2010) Artificial selection for determinate growth habit in soybean. Proceedings of the National Academy of Sciences 107:8563-8568. https://doi.org/10.1073/pnas.1000088107

Trapp JJ, Urrea CA, Zhou J, Khot LR, Sankaran S, Miklas PN (2016) Selective phenotyping traits related to multiple stress and drought response in dry bean. Crop Science 56:1460-1472. https://doi.org/10.2135/cropsci2015.05.0281

Turner S (2018) qqman: an R package for visualizing GWAS results using Q-Q and manhattan plots. Journal of Open Source Software 3:731.

USDA Economic Research Service (2013) Table 7. Certified organic beans. Acres of soybeans, dry beans, dry peas/lentils by state, 1997 and 2000-11.

Weller JL, Vander Schoor JK, Perez-Wright EC, Hecht V, González AM, Capel C, Yuste-Lisbona FJ, Lozano R, Santalla M (2019) Parallel origins of photoperiod adaptation following dual domestications of common bean. Journal of Experimental Botany 70:1209-1219. https://doi.org/10.1093/jxb/ery455

Woebbecke DM, Meyer GE, Von Bargen K, Mortensen DA (1995) Color indices for weed identification under various soil, residue, and lighting conditions. Transactions of the ASAE 38:259-269. https://doi.org/https://doi.org/10.13031/2013.27838

Xavier A, Hall B, Hearst AA, Cherkauer KA, Rainey KM (2017) Genetic architecture of phenomic-enabled canopy coverage in *Glycine max*. Genetics 206:1081-1089. https://doi.org/10.1534/genetics.116.198713

Zhao DL, Atlin GN, Bastiaans L, Spiertz JHJ (2006) Cultivar weed-competitiveness in aerobic rice: Heritability, correlated traits, and the potential for indirect selection in weed-free environments. Crop Science 46:372-380. https://doi.org/10.2135/cropsci2005.0192

Zhou J, Khot LR, Boydston RA, Miklas PN, Porter L (2018) Low altitude remote sensing technologies for crop stress monitoring: a case study on spatial and temporal monitoring of irrigated pinto bean. Precision Agriculture 19:555-569. https://doi.org/10.1007/s11119-017-9539-0

 doi:10.20944/preprints202004.0309.v1

Peer-reviewed version available at *Remote Sens.* **2020**, *12*, 1748; doi:10.3390/rs12111748

Figures:

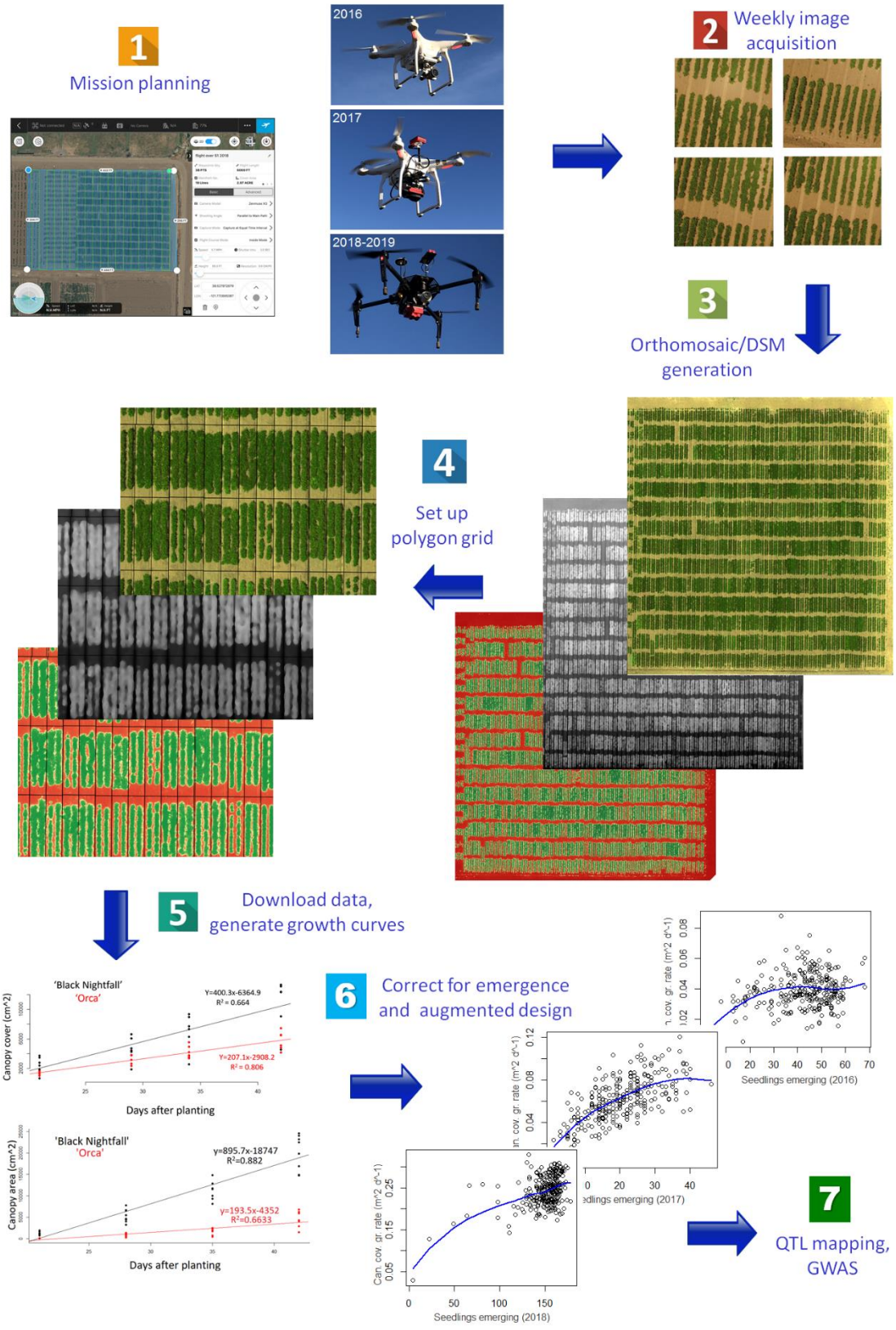

Figure 1: Phenotyping pipeline. 1) Experiment and mission planning. Flight were conducted using Map Pilot (2016), Atlas Flight (2017), and DJI Ground Station Pro (2018-2019) based on hardware compatibility. Aircraft and cameras included a DJI Phantom 3 Pro with stock RGB camera (2016), a DJI Phantom 3 Pro with a Parrot Sequoia multispectral camera (2017), and a DJI Matrice 100 with a RedEdge-M (2018-2019). 2) Field images were collected at 21, 28, 35, and 42 days after planting. 3) Orthomosaics and digital surface models were generated from raw images using Pix4Dmapper Pro. Vegetation indices, spatial classification layers, and masked orthomosaics were generated using the QGIS raster calculator function. 4) Shapefile grids were developed using the QGIS vector grid function. 5) Phenotype data were downloaded for each plot, which were used to develop growth curves. 6) Corrections for emergence and augmented design were performed in R. 7) Growth and canopy data were used as phenotype inputs for GWAS and QTL mapping.

Preprints (www.preprints.org) | NOT PEER-REVIEWED | Posted: 19 April 2020 doi:10.20944/preprints202004.0309.v1

Peer-reviewed version available at *Remote Sens.* **2020**, *12*, 1748; doi:10.3390/rs12111748

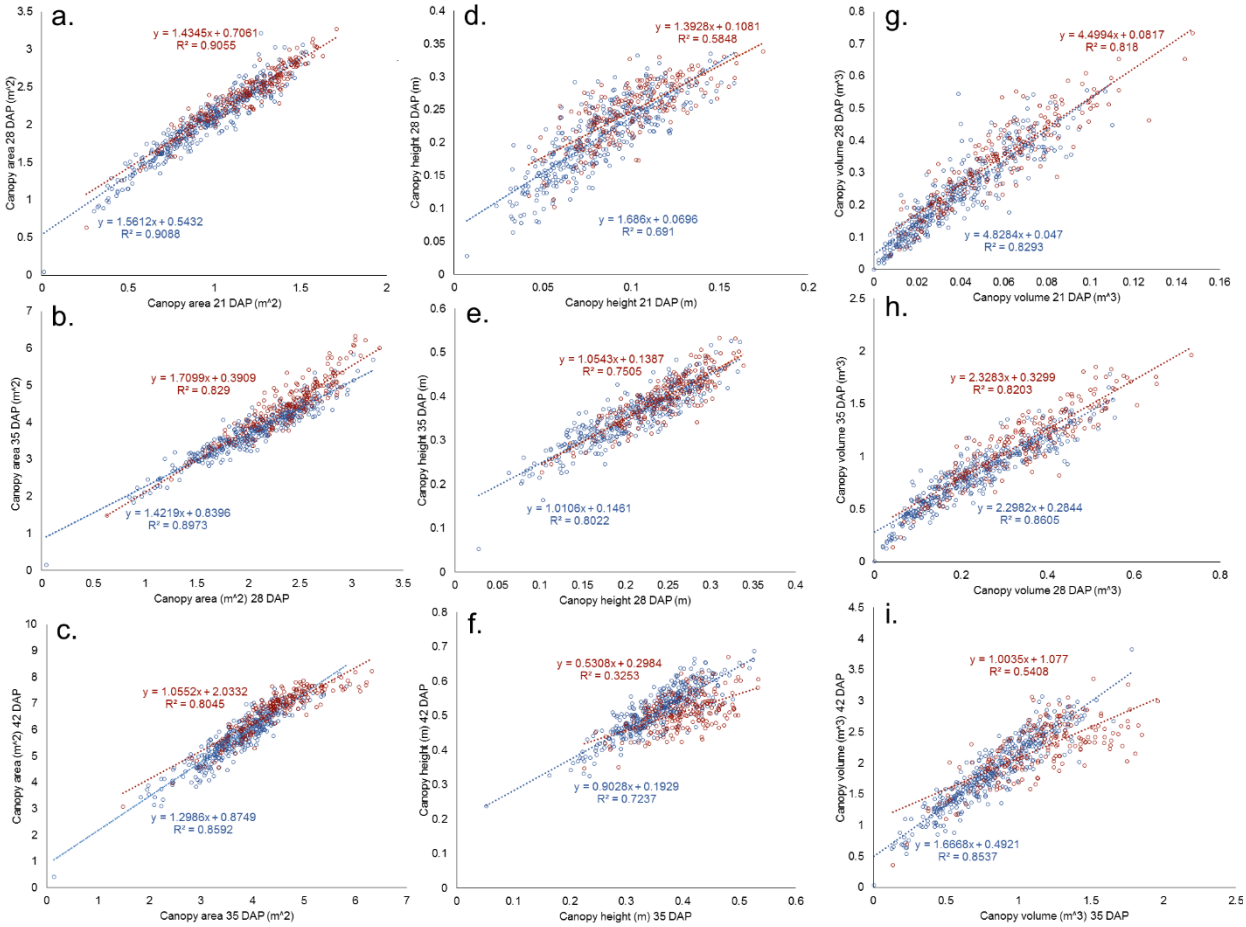

Figure 2: High-precision drone-based evaluation of canopy area, height, and volume leads to strong data reproducibility between weeks. SNP S07_34512442 on Pv07 was related to canopy area (a-c), height (d-f), and volume (g-i) in the MDP in 2018. Types with a thymine at this position (red) initially have greater canopy area and height than those with a guanine (blue) (a,d,g). By 42 DAP, varieties with a thymine at the position experience greater lodging, reducing the rate of canopy height (f) and volume increase (i).

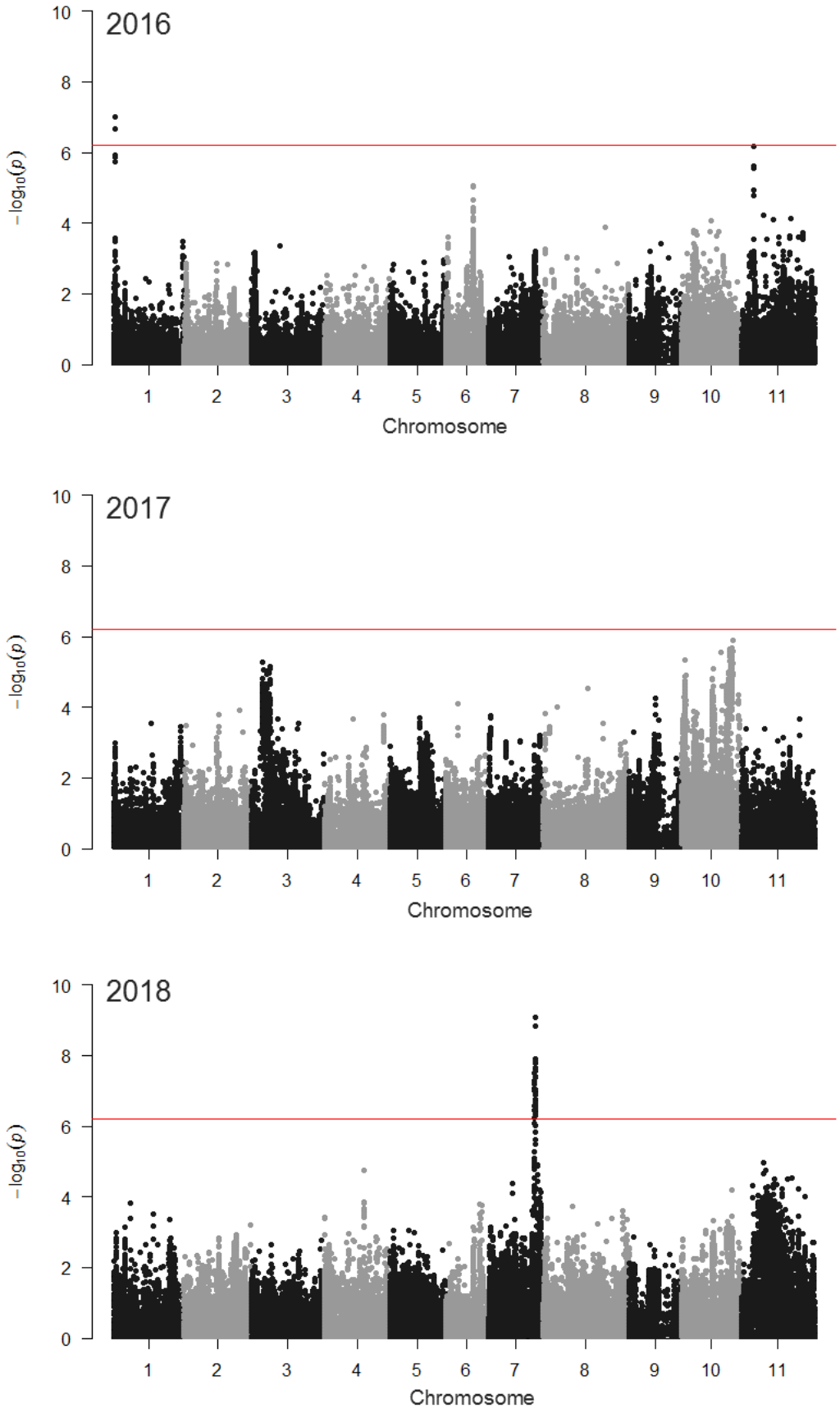

Figure 3: MDP canopy cover growth rate 21-42 DAP, emergence correction by LOESS residuals. Significant SNPs were found on different chromosomes in each year, reflecting the complex interactions between genotype and environment for canopy cover growth rate. By far the most significant SNPs from any year were identified in 2018. The most significant SNP (Pv07 position 34,512,442) is found in the 5' UTR of Phvul.007G221800, a gene model that has been postulated to pleiotropically affect canopy architecture, height, and lodging (Moghaddam et al. 2016). GWAS was conducted as general linear model in TASSEL with a 81K SNP set, correction for emergence by residuals from a LOESS model of growth rate as function of emergence. The red lines indicate a Bonferroni-corrected significance threshold (LOD=6.21).

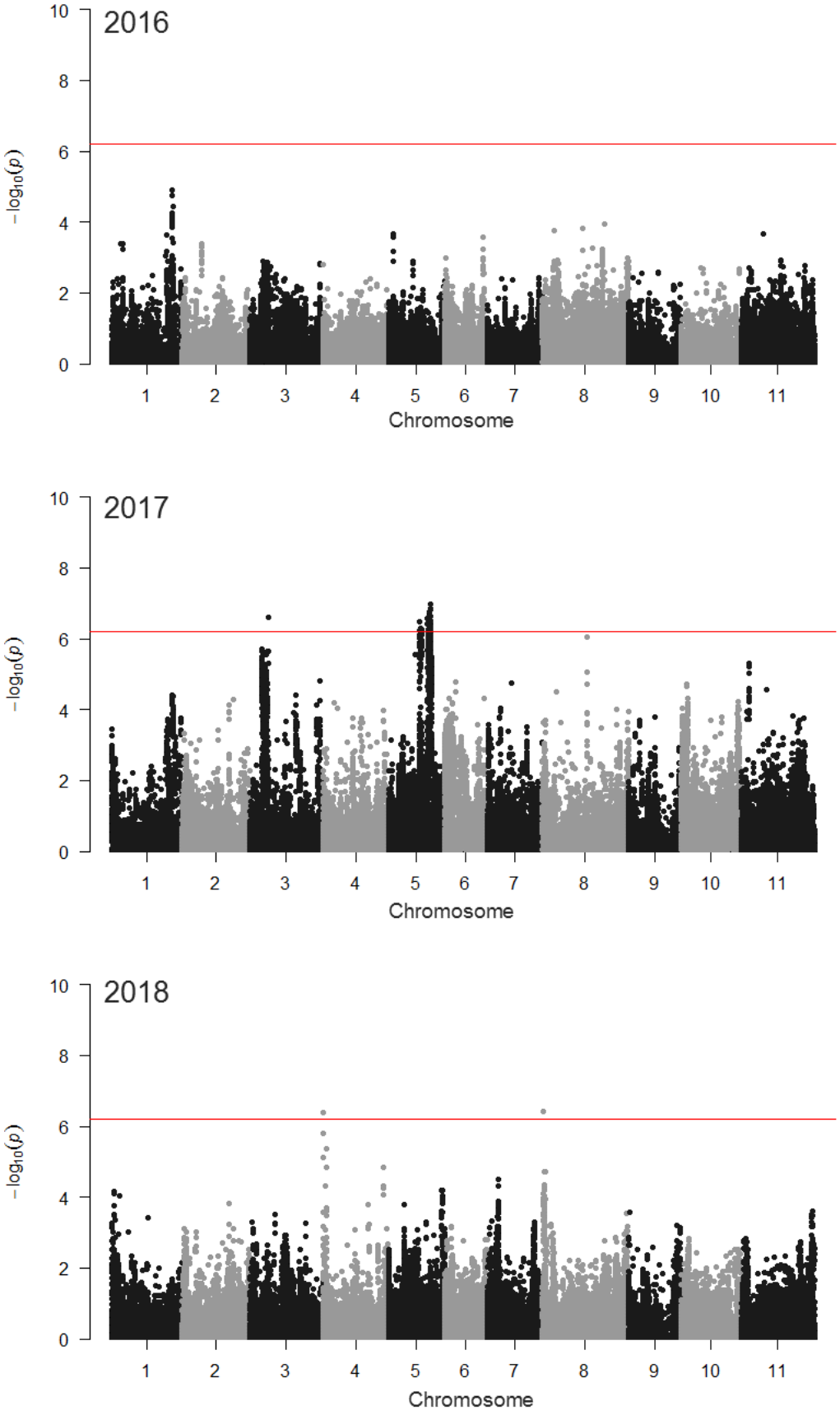

Figure 4: Drone-measured maximum canopy height GWAS. The most significant SNPs in 2016 are clustered near *PvTFL1y* on chromosome Pv01. The most significant SNPs in 2018 are found on Pv04, near a canopy height QTL identified by Moghaddam et al. (2016). No correction for augmented design was implemented. GWAS was conducted as general linear model in TASSEL with a 81K SNP set. The red lines indicate a Bonferroni-corrected significance threshold (LOD=6.21).

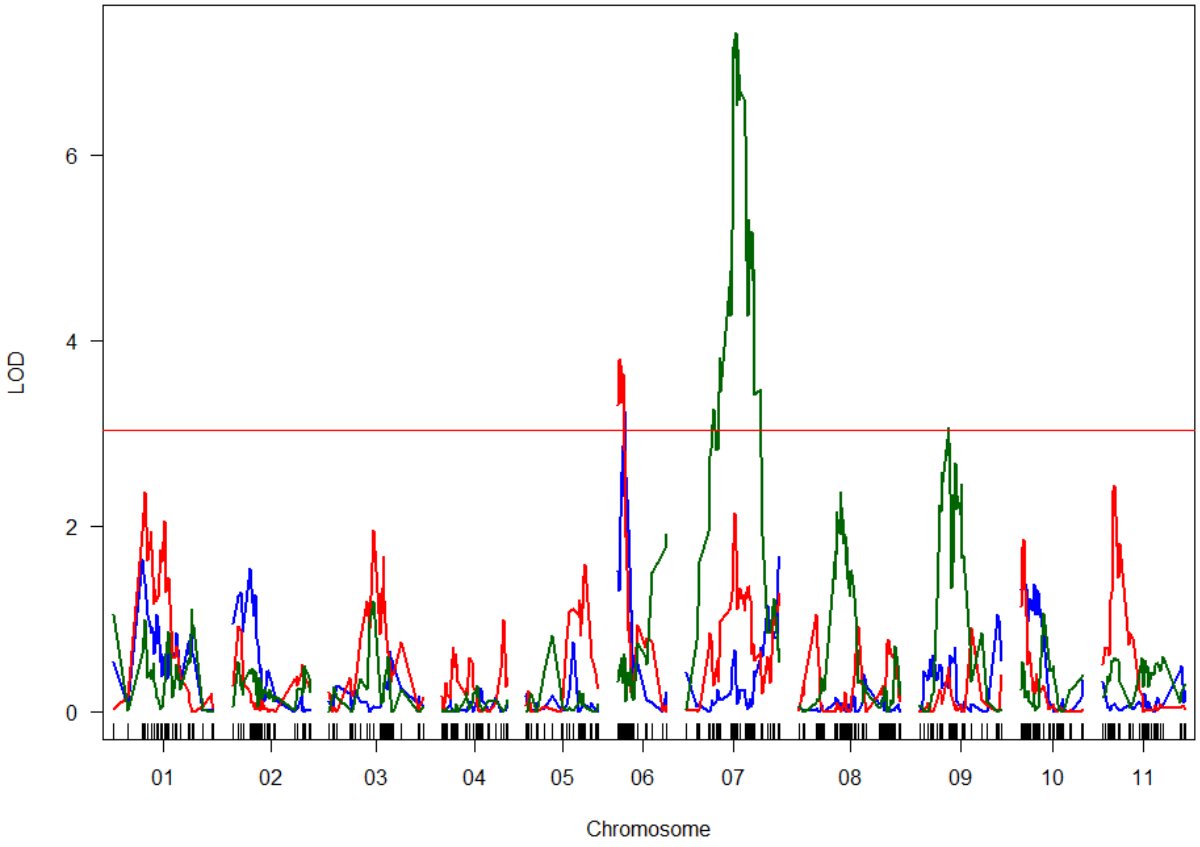

Figure 5: QTL mapping of canopy area growth rate in the BxO population in 2017 (blue), 2018 (red), and 2019 (green), with LOESS residuals used as correction for emergence. Major QTLs exist on chromosomes Pv06, Pv07, and Pv09. Growth rate is strongly influenced by environment, leading to different QTLs controlling the trait among years. The chromosome Pv07 QTL is found on the same chromosome arm as the most significant SNP from the GWAS of the MDP. The underlying gene may be pleiotropically related to canopy architecture, height, and lodging. Plots were four-fold larger in 2019 than in previous years, potentially leading to improved QTL resolution. Results based on slope of canopy cover increase between 21, 28, 35, and 42 days after planting, with a residual-based correction for a LOESS model of emergence rate and a correction for augmented design. The 95th percentile of LOD scores from 1000 randomized permutations of the data (LOD=3.03) was used as a significance threshold.

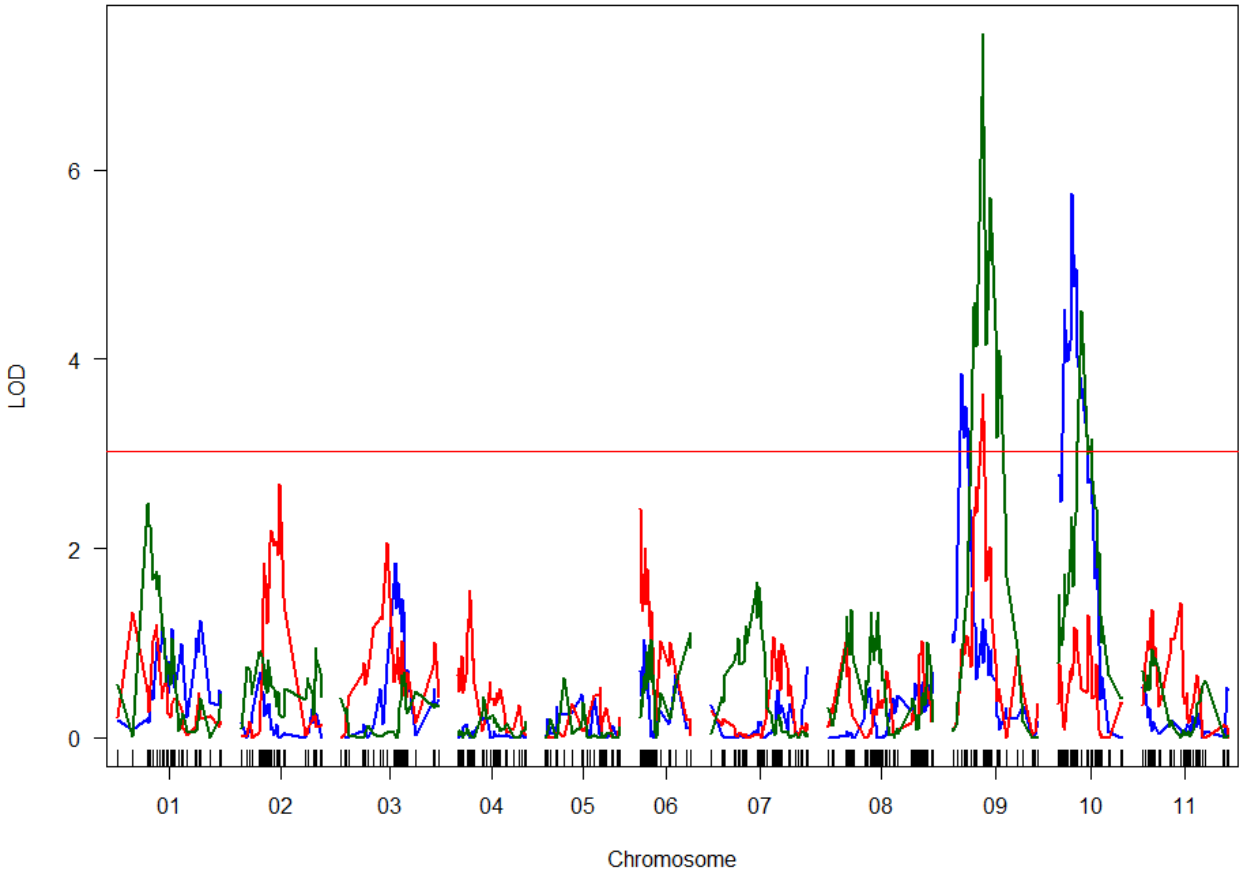

Figure 6: QTL mapping of drone-measured maximum canopy height 42 days after planting in 2017 (blue), 2018 (red), and 2019 (green). QTLs on Pv09 are related to maximum canopy height in all three years, whereas QTLs on Pv10 are responsible for the trait in two years. The same Pv09 SNPs were most significant in 2018 and 2019. No correction for augmented design was implemented. The 95th percentile of LOD scores from 1000 randomized permutations of the data (LOD=3.03) was used as a significance threshold.

Table 1. UAV phenotyping information.

Year of trial	Population evaluated	Aircraft	Primary camera	Camera type	Altitude	Mission planning application	GSD
2016	MDP	DJI Phantom 3 Professional	Stock (Sony EXMOR 1/2.3 sensor)	RGB	17m	Map Pilot	0.7cm/px
2017*	MDP, BxO	DJI Phantom 3 Professional	Parrot Sequoia	Multi-spectral	20m	Atlas Flight	1.9cm/px
2018	MDP, BxO	DJI Matrice 100	Micasense RedEdge-M	Multi-spectral	20m	DJI GS Pro	1.4cm/px
2019	BxO	DJI Matrice 100	Micasense RedEdge-M	Multi-spectral	20m	DJI GS Pro	1.4cm/px

*The first flight of 2017 (21 DAP) used the materials and methods of 2016.

Preprints (www.preprints.org) | NOT PEER-REVIEWED | Posted: 19 April 2020 doi:10.20944/preprints202004.0309.v1

Peer-reviewed version available at *Remote Sens.* **2020**, *12*, 1748; doi:10.3390/rs12111748

Supplemental Information

Supplemental Figures:

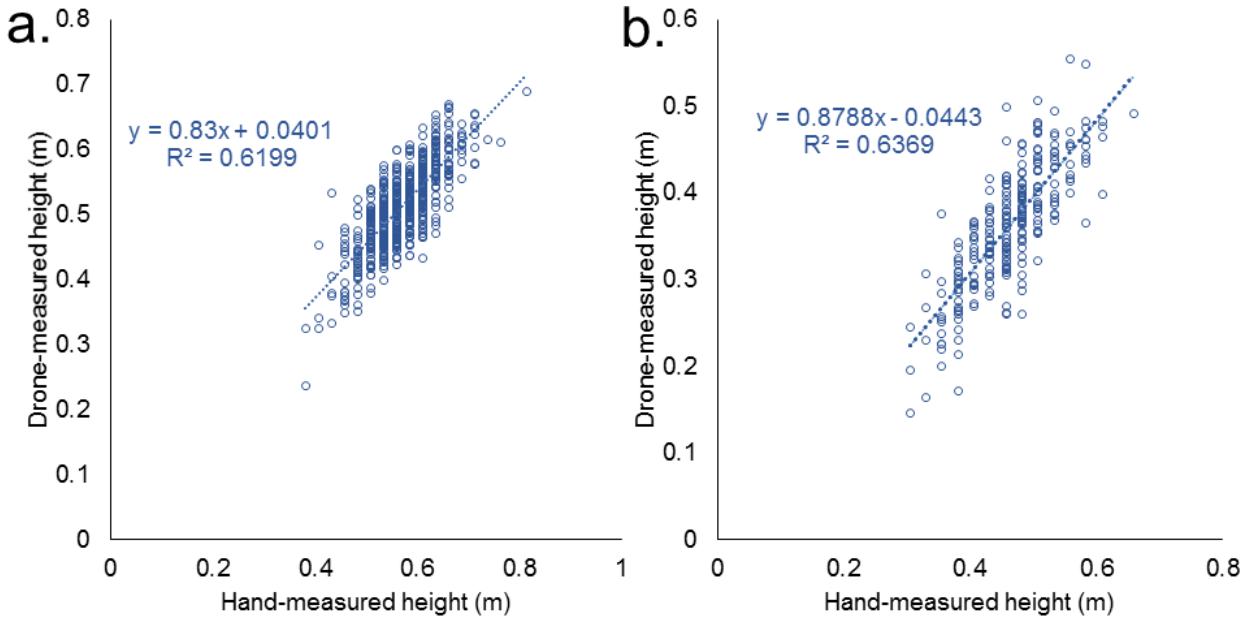

Figure S1: Correlation between hand-measured and drone-measured canopy heights at 42 DAP in A) the Middle American Diversity panel, 2018, and B) the BxO recombinant inbred population, 2019.

 doi:10.20944/preprints202004.0309.v1

Peer-reviewed version available at *Remote Sens.* **2020**, *12*, 1748; doi:10.3390/rs12111748

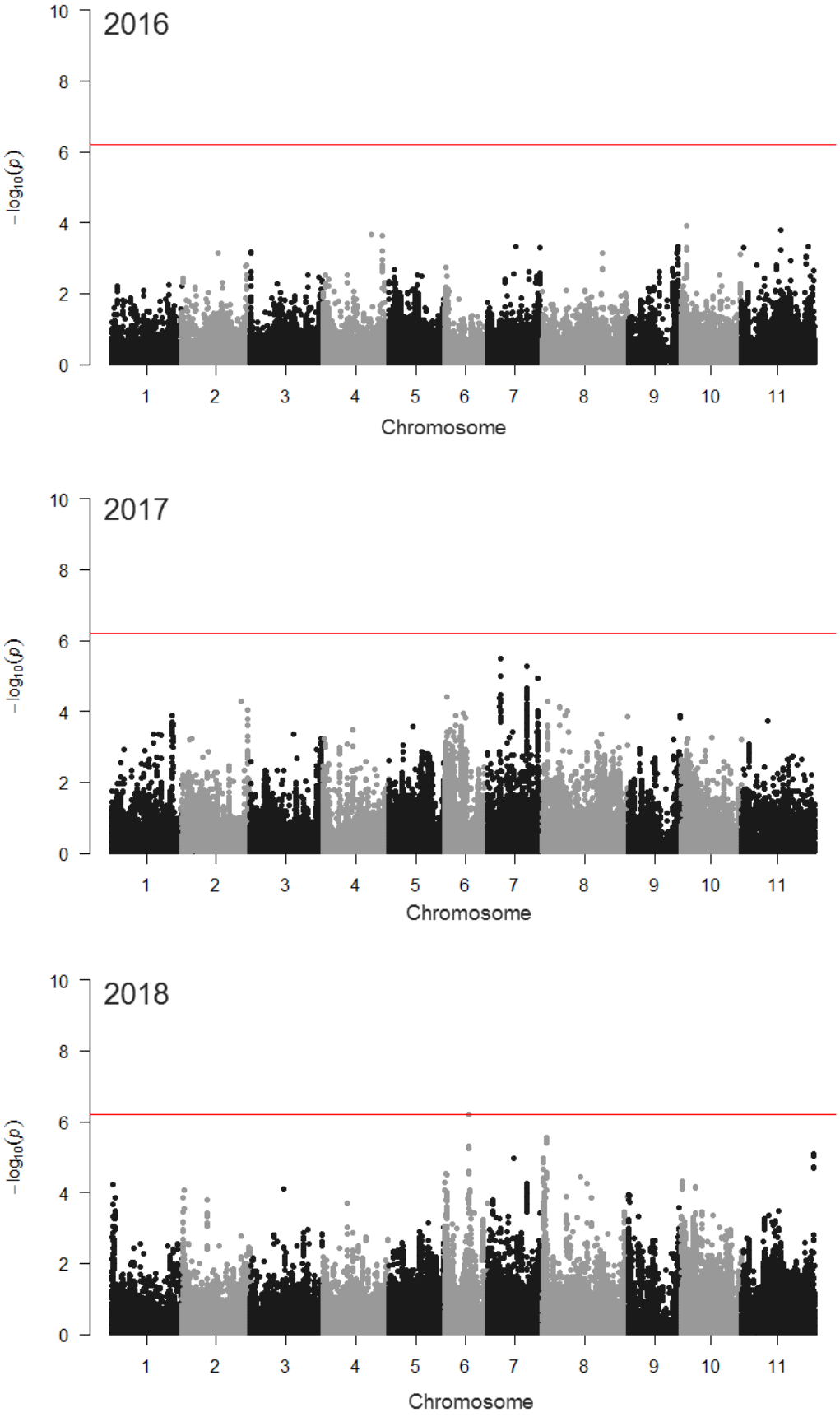

Figure S2: GWAS of seedling emergence rate in the Middle American Diversity panel. A SNP on Pv06 (LOD=6.19) approached significance based on a conservative Bonferroni threshold (LOD=6.21) of 2018 data. GWAS conducted in TASSEL based on a general linear model through the SNiPlay interface.

Preprints (www.preprints.org) | NOT PEER-REVIEWED | Posted: 19 April 2020 doi:10.20944/preprints202004.0309.v1

Peer-reviewed version available at *Remote Sens.* **2020**, *12*, 1748; doi:10.3390/rs12111748

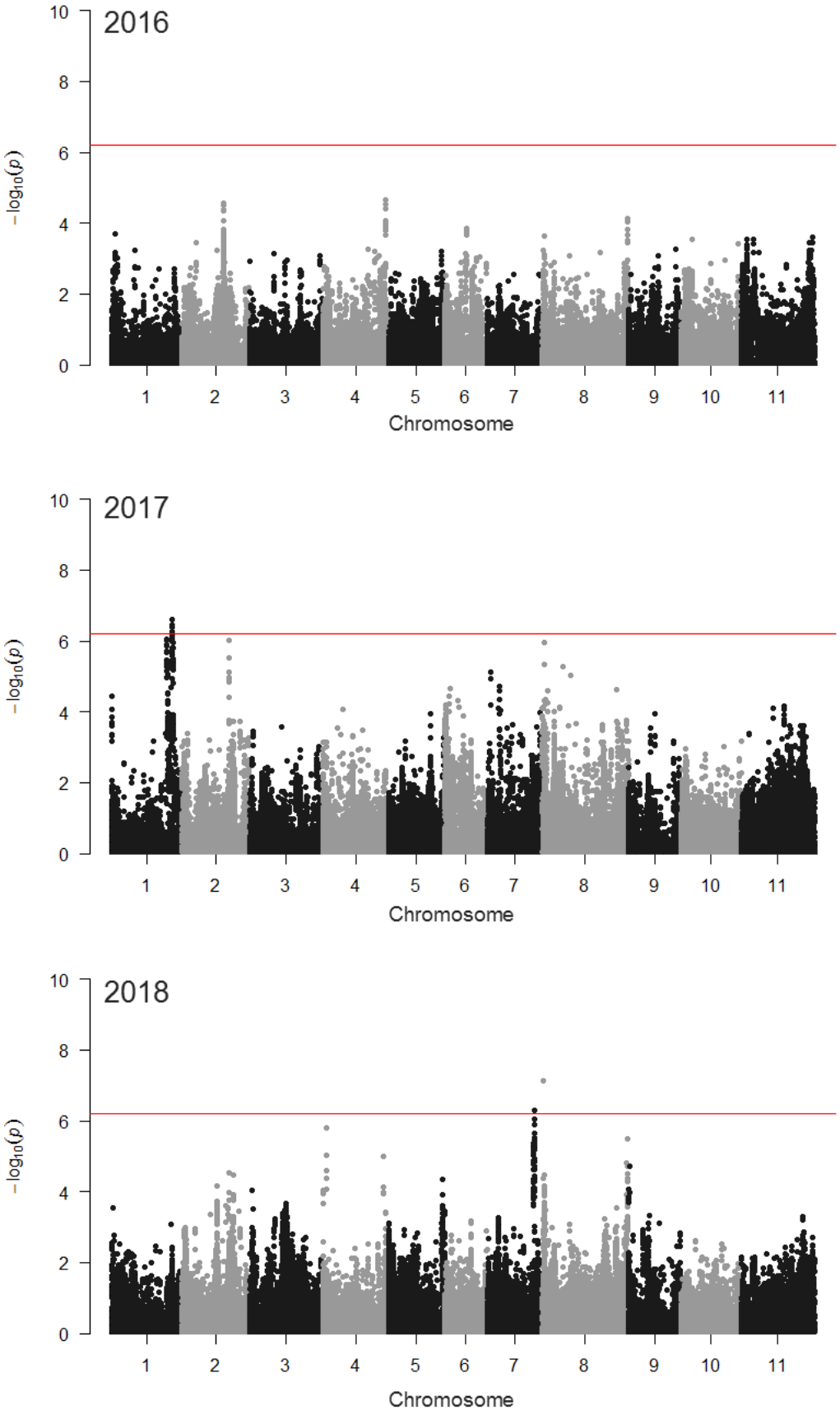

Figure S3: Hand-measured canopy height GWAS in the MDP. In 2017, a significant QTL was identified near PvTFL1y on chromosome Pv01. In 2018, the Pv07 locus associated with growth rate was also associated with hand-measured canopy height. GWAS conducted in TASSEL based on a general linear model through the SNiPlay interface.

Preprints (www.preprints.org) | NOT PEER-REVIEWED | Posted: 19 April 2020 doi:10.20944/preprints202004.0309.v1

Peer-reviewed version available at *Remote Sens.* **2020**, *12*, 1748; doi:10.3390/rs12111748

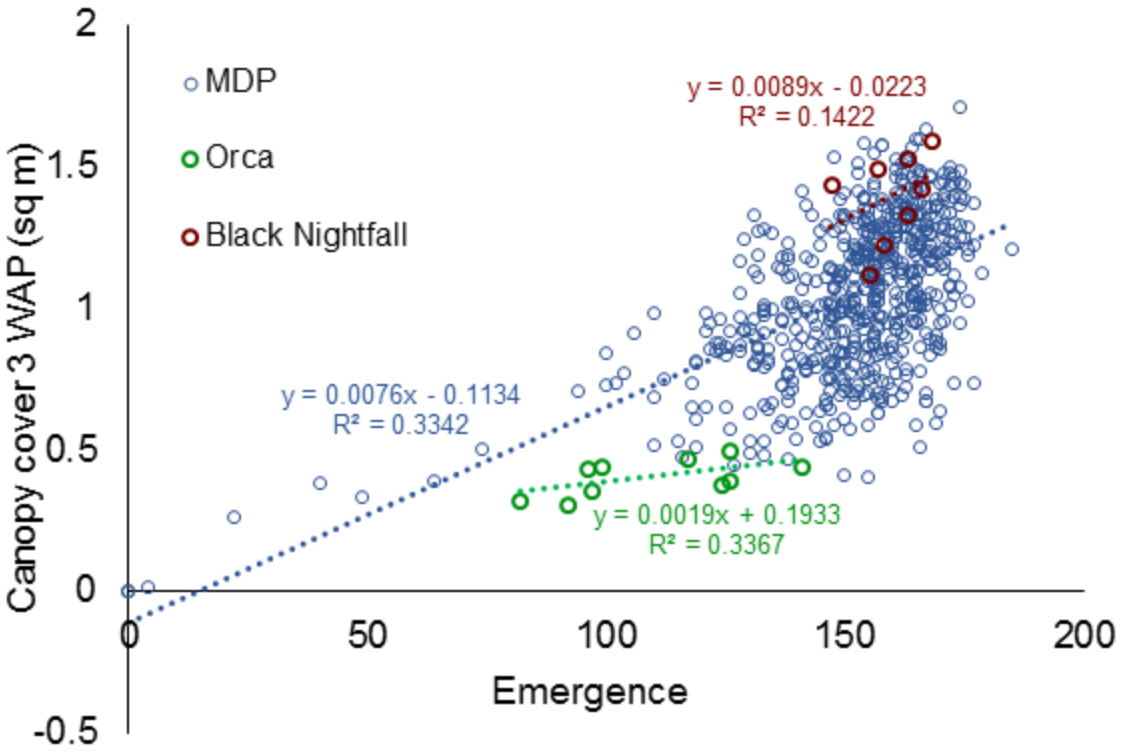

Figure S4: 2018 emergence and growth rate in the Middle American diversity panel, including Black Nightfall and Orca plots as controls. The x axis represents the number of seeds germinated out of 180 seeds planted. Black Nightfall has stronger seedling emergence, and above-average growth rates, even after emergence correction. Orca has lower emergence, and below-average growth rates relative to types with similar emergence rates.

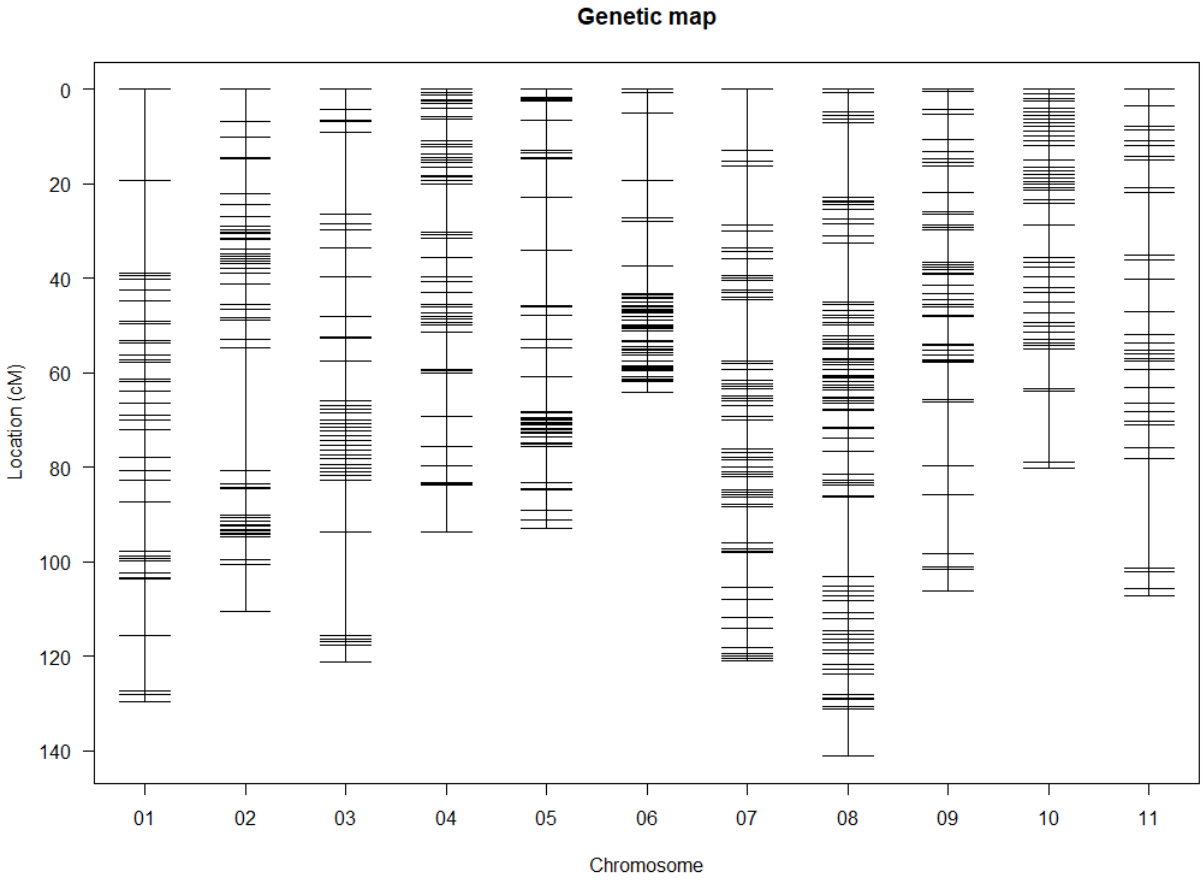

Figure S5: Black Nightfall x Orca (BxO) population linkage map: Linkage groups (vertical lines) were ordered and oriented to correspond with the 11 chromosomes of the common bean reference genome (Pedrosa-Harand et al. 2008). A total of 730 markers (horizontal bars) were distributed across 1138cM of recombination space.

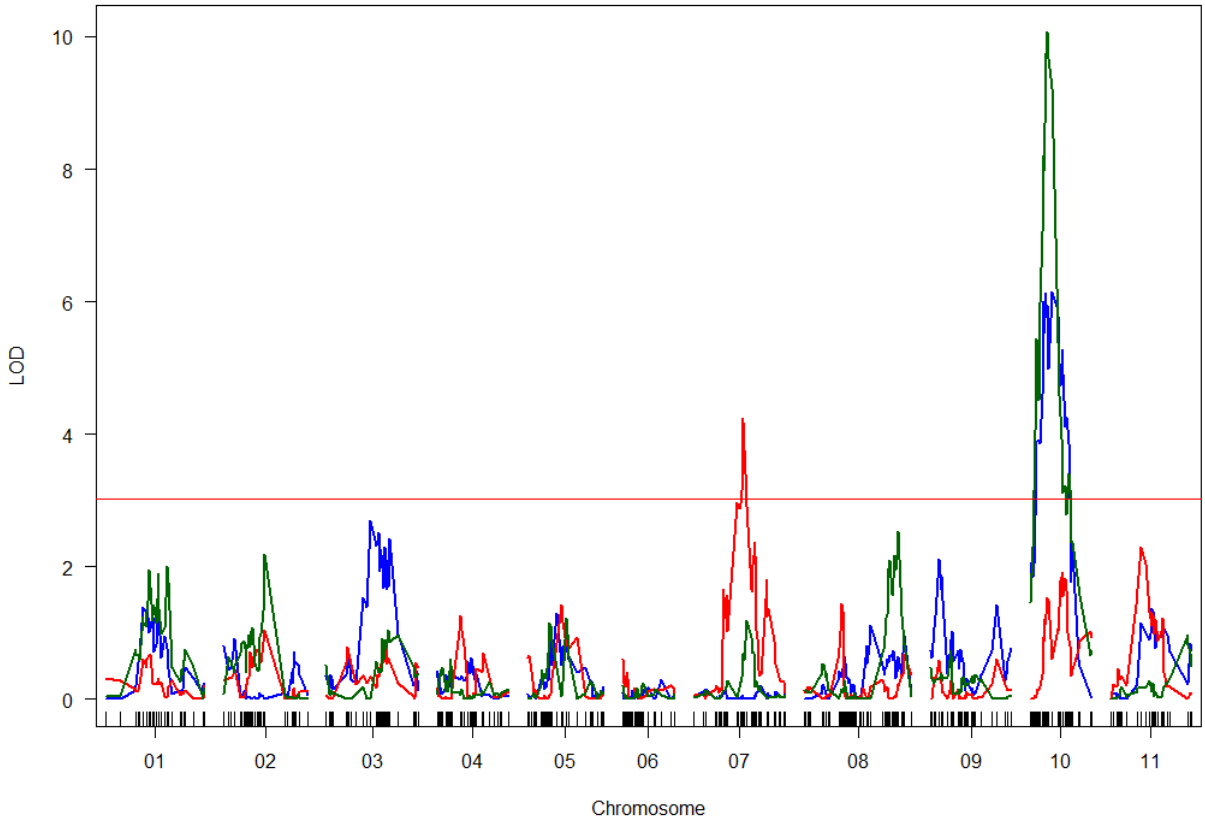

Figure S6: QTLs related to emergence rate. Robustness of germination and emergence has a profound effect on canopy growth. Emergence was low in 2017 (32%, blue) and 2019 (61%, green), but relatively high in 2018 (85%, red), and different QTLs controlled the trait between these years. The 95th percentile of LOD scores from 1000 randomized permutations of the data (LOD=3.03) was used as a significance threshold.

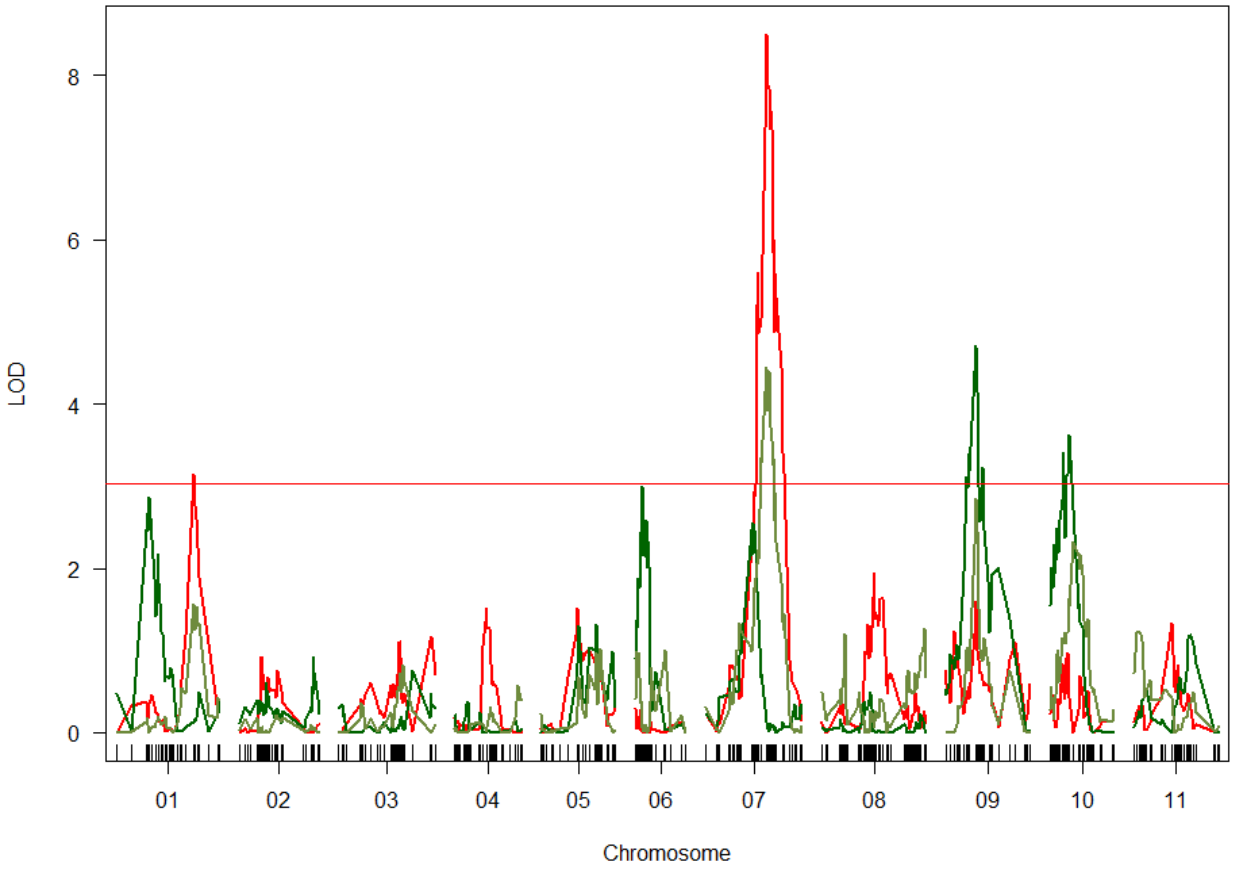

Figure S7: QTL mapping of hand-measured heights in the BxO population. At 42 DAP in 2018 (red), a major peak on Pv07 was evident. At 42 DAP in 2019 (dark green), several smaller QTLs were related to the trait, but by 63 DAP (light green), the Pv07 QTL had become significant as plants began to lodge. Results were based on data without correction for augmented design. The 95th percentile of LOD scores from 1000 randomized permutations of the data (LOD=3.03) was used as a significance threshold.

Supplemental Tables.

Table S1: Summary of QTLs significantly associated with growth rate in the BxO RI population. The most significant SNP(s) are listed along with the most significant SNP in the upstream and downstream directions. SNP coordinates are based on v2.1 of the *Phaseolus vulgaris* genome. QTLs with identical positions between traits or years are indicated with asterisks in the chromosome column.

Trait	Year	Chromosome	Most significant SNP	Position of most significant SNP (bp, genome v2.1)	LOD score, most significant SNP	Upstream flanking SNP	Position of flanking SNP 1 (Mb, genome v2.1)	LOD score, flanking SNP 1	Downstream flanking SNP	Position of flanking SNP 2 (Mb, genome v2.1)	LOD score, flanking SNP 2
Emergence	2017	Pv10**	sc00119ln552178_356133_C_T_101986727	39124986	6.17	sc01321ln86834_2687_G_A_343229024	33609458	6.12	sc00156ln490745_316806_T_G_121001808	39812966	5.88
Emergence	2018	Pv07***	sc01522ln71313_49907_C_T_359138275, sc00659ln174637_29312_T_G_262099636	26581201, 26781502	4.25	sc00667ln172407_43926_G_A_263503992	25530277	3.15	sc00403ln261324_207173_G_A_207343141	26871528	4.19
Emergence	2019	Pv10	sc02147ln44740_15412_C_T_394527222	35632623	10.06	sc00603ln190994_176505_G_A_252033814	35357895	9.73	sc00078ln669540_46230_G_T_76714253	36893960	9.71
Canopy height, hand-measured 42 DAP	2018	Pv01	sc00022ln1003704_280981_C_T_32782853	48773773	3.14	sc01259ln90943_48696_C_T_337774864	47084408	1.19	sc00022ln1003704_178718_A_G_32680590	48872687	3.06
Canopy height, hand-measured 42 DAP	2018	Pv07	sc00262ln351368_226896_C_T_164426117	32298702	8.5	sc01434ln78222_42548_A_C_352565471	32135594	8.15	sc00394ln266395_179893_C_A_204933545	32612675	8.36
Canopy height, hand-measured 42 DAP	2019	Pv09	sc00105ln590179_378162_T_G_94032280, sc00105ln590179_432554_A_G_94086672	17007673, 16953589	4.71	sc00080ln658250_291062_G_A_78288301	14192463	3.18	sc00063ln704677_263799_C_T_66628438	17719599	4.67
Canopy height, hand-measured 42 DAP	2019	Pv10	sc01142ln101735_70111_C_A_326510153, sc00633ln181418_21828_T_C_257467034	37228017, 37683218	3.63	sc00078ln669540_46230_G_T_76714253	36893960	3.63	sc00119ln552178_356133_C_T_101986727	39124986	2.72
Canopy height, hand-measured 63 DAP	2019	Pv07	sc01434ln78222_42548_A_C_352565471	32135594	4.44	sc00138ln510194_187113_A_C_111872296	30152459	3.35	sc00262ln351368_226896_C_T_164426117	32298702	4.44
Canopy height, drone-measured 42 DAP	2017	Pv09	sc00016ln1258381_85213_A_C_25771824	8427110	3.85	sc01015ln116554_82418_G_A_312723529	6088874	2.04	sc00042ln819284_180429_C_T_50792076	10109240	3.5
Canopy height, drone-measured 42 DAP	2017	Pv10	sc00267ln345535_21418_A_G_165965167, sc00794ln147497_57984_G_T_283720856	8184240, 8060803	5.73	sc04617ln9320_7677_T_C_450621006	5625057	4.52	sc01197ln96689_83817_G_A_331981619	9179745	5.76
Canopy height, drone-measured 42 DAP	2018	Pv09*	sc00105ln590179_378162_T_G_94032280, sc00105ln590179_432554_A_G_94086672	17007673, 16953589	3.63	sc00080ln658250_129523_C_T_78126762	14034332	2.65	sc00063ln704677_337006_T_C_66701645	17650074	3.34
Canopy height, drone-measured 42 DAP	2019	Pv09*	sc00105ln590179_378162_T_G_94032280, sc00105ln590179_432554_A_G_94086672	17007673, 16953589	7.44	sc00324ln307318_256674_A_G_184899333	13555560	4.6	sc00105ln590179_155124_C_A_93809242	17226788	6.93
Canopy height, drone-measured 42 DAP	2019	Pv10**	sc00119ln552178_356133_C_T_101986727	39124986	4.51	sc00078ln669540_46230_G_T_76714253	36893960	3.13	sc00156ln490745_316806_T_G_121001808	39812966	3.18

Canopy cover growth rate, emergence corrected by Loess residuals	2017	Pv06	sc00162ln482802_46418_G_A_123659537	19950405	3.28	sc00534ln209932_154675_C_A_238084299	19359174	2.86	sc00827ln142080_1193_C_T_288452244	20003376	3.24
Canopy cover growth rate, emergence corrected by Loess residuals	2018	Pv06	sc00630ln182007_6318_T_C_256906010	17062325	3.8	sc00734ln158067_119101_A_G_274625952	16591001	3.78	sc01288ln88608_79400_A_G_340410560	17688533	3.74
Canopy cover growth rate, emergence corrected by Loess residuals	2019	Pv07***	sc01522ln71313_49907_C_T_359138275, sc00659ln174637_29312_T_G_262099636	26581201, 26781502	7.32	sc03437ln19680_9381_G_A_433942786	22404289	7.23	sc00403ln261324_207173_G_A_207343141	26871528	7.25
Canopy cover growth rate, emergence corrected by Loess residuals	2019	Pv09*	sc00105ln590179_378162_T_G_94032280, sc00105ln590179_432554_A_G_94086672	17007673, 16953589	3.06	sc00080ln658250_229923_A_C_78227162	14130721	2.57	sc00105ln590179_155124_C_A_93809242	17226788	2.94

Table S2: A comparison of early-season growth between Black Nightfall (BN) and Orca.

Trait	Year	mean (BN)	mean (Orca)	SD (BN)	SD (Orca)	p-value (two-tailed t-test)	Significance
Emergence	2016	44.83	41.33	12.90	11.59	0.66	ns
Emergence	2017	26.38	12.75	6.39	7.07	0	**
Emergence	2018	159.63	109.88	6.36	19.19	0	***
Emergence	2019	84.08	57.17	14.76	10.69	0	***
Canopy growth rate per plot (cm^2 plot $^{-1}$ day^{-1})	2016	480.43	281.91	135.82	52.29	0.01	**
Canopy growth rate per plot (cm^2 plot $^{-1}$ day^{-1})	2017	994.19	213.31	174.33	89.61	0	***
Canopy growth rate per plot (cm^2 plot $^{-1}$ day^{-1})	2018	2807.86	1628.28	142.27	167.67	0	***
Canopy growth rate per plot (cm^2 plot $^{-1}$ day^{-1})	2019	2632.23	758.44	536.54	257.82	0	***
Canopy growth rate per plant (cm^2 $plant^{-1}$ day^{-1})	2016	10.91	7.57	1.58	2.89	0.047	*
Canopy growth rate per plant (cm^2 $plant^{-1}$ day^{-1})	2017	38.71	18.47	7.67	5.62	0	***
Canopy growth rate per plant (cm^2 $plant^{-1}$ day^{-1})	2018	17.60	15.26	0.78	2.96	0.06	ns
Canopy growth rate per plant (cm^2 $plant^{-1}$ day^{-1})	2019	31.73	13.26	5.80	3.67	0	***

Drone-measured canopy height 42 DAP (cm)	2016	13.1	10.0	4.6	2.7	0.19	ns
Drone-measured canopy height 42 DAP (cm)	2017	30.2	9.2	6.2	3.4	0	***
Drone-measured canopy height 42 DAP (cm)	2018	45.4	36.2	3.0	3.0	0	***
Drone-measured canopy height 42 DAP (cm)	2019	45.0	23.5	3.1	5.5	0	***
Hand-measured canopy height 42 DAP (cm)	2016	38.31	28.15	2.46	2.94	0	***
Hand-measured canopy height 42 DAP (cm)	2017	49.37	39.29	1.35	1.65	0	***
Hand-measured canopy height 42 DAP (cm)	2018	51.60	43.66	2.00	2.61	0	***
Hand-measured canopy height 42 DAP (cm)	2019	50.80	33.76	5.58	2.29	0	***

Table S3: Positions of SNPs significantly associated with traits through GWAS.

Trait	Year	Chromosome	Position, most significant SNP	LOD, most significant SNP
Canopy height, hand-measured 42 DAP	2017	Pv01	44777278	7.03
Canopy height, hand-measured 42 DAP	2018	Pv07	34462447	6.29
Canopy height, hand-measured 42 DAP	2018	Pv08	1316948	7.14
Canopy height, drone-measured 42 DAP	2017	Pv03	13349070	6.62
Canopy height, drone-measured 42 DAP	2017	Pv05	30689797	6.99
Canopy height, drone-measured 42 DAP	2018	Pv04	55103	6.39
Canopy height, drone-measured 42 DAP	2018	Pv08	1316948	6.42
Canopy cover growth rate, emergence corrected by LOESS residuals	2016	Pv01	1177020	7.01
Canopy cover growth rate, emergence corrected by LOESS residuals	2018	Pv07	34512442	9.08